EAGE

Fr CO2 P05

# Bayesian Inference In CO2 Storage Monitoring: A Way To Assess Uncertainties In Geophysical Inversions

B. Dupuy[1]*, A. Romdhane[1], P. Eliasson[1]
[1]SINTEF

## Summary

We present an integrated methodology for quantitative CO2 monitoring using Bayesian formulation. A first step consists in full-waveform inversion and CSEM inversion solved with gradient-based inverse methods. Uncertainty assessment is then carried out using a posteriori covariance matrix analysis to derive velocity and resistivity maps with uncertainty. Then, rock physics inversion is done with semi-global optimisation methodology and uncertainty is propagated with Bayesian formulation to quantify the reliability of the final CO2 saturation estimates.

## Introduction

For large-scale $CO_2$ storage projects, international regulations require setting up a suitable MMV (Measurement, Monitoring and Verification) plan. A monitoring plan is divided into three parts: containement, conformance and contingency. Conformance monitoring requires matching modelled previsions and monitoring measurements. Such comparisons are carried out based on some measurable quantities that can be derived by geophysical measurements. Typically, seismic and/or CSEM (Controlled Source ElectroMagnetic) surveys associated with proper imaging methods allow to derive $CO_2$ saturations or other relevant rock physics properties (Ghosh et al., 2015; Dupuy et al., 2017). Quantitative geophysical imaging uses a combination of inversion methodologies (Dupuy et al., 2016). Proper conformance monitoring requires estimation of relevant susbsurface quantities (such as $CO_2$ saturations). The inverse problems associated with the first (geophysical inversion) or second step are however non-linear, highly undetermined and non-unique. Uncertainty evaluation is therefore of critical importance. Both inversions are based on Bayesian formulation (Tarantola, 2005). The first inversion step is carried out with gradient-based local optimization while the second inversion step consists in a deterministic global optimization. We propose in this work to integrate the two inversion steps to propagate uncertainty estimated in the first step to the second inversion step.

## Inversion formulation

Bayesian formulation of geophysical inverse problems is extensively described by Tarantola (2005). Based on Bayes theorem, the solution of the inverse problem can be described by a general formulation calculating the posterior probability distribution $\boldsymbol{\sigma}_{post}$ of the model $\boldsymbol{m}$ such as:

$$\boldsymbol{\sigma}_{post} = c\boldsymbol{\rho}_{prior}(\boldsymbol{m})L(\boldsymbol{m}|\boldsymbol{d}_{obs}) \ , \tag{1}$$

where $c$ is a constant, $\boldsymbol{\rho}_{prior}(\boldsymbol{m})$ is the prior probability density function of model $\boldsymbol{m}$ and $L(\boldsymbol{m}|\boldsymbol{d}_{obs})$ is the data likelihood misfit function describing the discrepancy between observed data $\boldsymbol{d}_{obs}$ and modelled data $g(\boldsymbol{m})$ ($\boldsymbol{m}$ being the model vector and $g$ being the forward model operator used to calculate modelled data). Both inversion steps of our quantitative imaging workflow are using Bayesian formulation. The first inversion step uses waveform-based imaging methodologies, for instance Full Waveform Inversion (FWI) for seismic data. The forward problem consists in solving the wave equation for a given mode (acoustic, elastic, viscoelastic, etc). The associated inverse problem aims at minimizing the discrepancy between modeled and observed data. It can be derived in a least square sense and iteratively solved with a preconditioned gradient algorithm (Romdhane and Querendez, 2014). Uncertainty analysis can be performed based on the computation of the inverse of the Hessian, which can be interpreted as posterior covariance matrix in a local probabilistic sense (Eliasson and Romdhane, 2017). It allows generation of a set of equivalent models, all explaining similarly well the observed data.

The second inversion step consists in the extraction of relevant rock physics property models from the derived seismic attributes. Similarly to the first step, a data fitting process is carried out between modelled rock physics properties and observed data. The forward problem is defined by a rock physics model, that should be calibrated or generic enough to be applicable to the dataset. In the following examples, we use Biot-Gassmann (Biot, 1956; Gassmann, 1951) rock physics models coupled with the estimation of an effective fluid phase by Brie equation (Brie et al., 1995). Given the low computational requirement of the forward model, the inverse problem can be solved with global or semi-global optimization algorithms such as Monte-Carlo or Neighourhood Algorithm (NA) (Sambridge, 1999a). We used NA to estimate $CO_2$ saturation at Sleipner (Dupuy et al., 2017). In this case, the discrepancy between modelled data $g(\boldsymbol{m})$ ($\boldsymbol{m}$ being the model vector and $g$ being the rock physics model set of equations) and observed data $\boldsymbol{d}_{obs}$ was formulated with a scalar function $C(\boldsymbol{m})$ following L2 norm. We update this L2 norm formulation to add data covariance matrix $\boldsymbol{C_D}$ describing noise statistics in input data such as:

$$C(\boldsymbol{m}) = \left[(\boldsymbol{d}_{obs} - g(\boldsymbol{m}))^T \ \boldsymbol{C_D}^{-1} \ (\boldsymbol{d}_{obs} - g(\boldsymbol{m}))\right] \ . \tag{2}$$

The data covariance matrix (or prior data covariance) in this second step will be described by the posterior covariance matrix analysis carried out in the first step. Concretely, a velocity model with uncertainty

(standard deviation) will be derived in the first inversion step and this velocity data +/- uncertainty will be used as input in the second inversion step. We will compare results of derived rock physics properties taking into account this prior data uncertainty or not.

Other on-going updates in the rock physics inversion step are not shown in this abstract. Spatial correlation between data points (to avoid checkerboard patterns) is implemented and currently tested via global inversion of all data points in one system instead of independent inversions for each data point. In addition, measurement of correlation and trade-off of any ensemble of inverted models (such as the ensemble of models derived by NA) can be done a posteriori using the algorithm proposed by Sambridge (1999b). Approximate posterior probability density is defined and importance sampled to calculate Bayesian integrals such as posterior mean models and covariance matrices, resolution matrices and marginal distributions. Prior model probability distribution can be easily considered in this post-Bayesian analysis.

**Case study for propagation of uncertainty**

We consider a synthetic example representing Sleipner Utsira data (Dupuy et al., 2017), using acoustic FWI results (P-wave velocity) and CSEM inversion results (resistivity). Prior (constant) rock physics properties are defined from log data, laboratory measurements and regional geology knowledge. We show examples for baseline (before $CO_2$ injection, 1994 vintage) and monitor datasets (2008 vintage). Before injection, we focus the rock physics inversion on rock frame properties, i.e. dry bulk modulus, dry shear modulus and porosity. After injection, we assume that the rock frame properties are unchanged and that the geophysical attributes are sensitive only to the fluid phase change i.e. $CO_2$ saturation and the way the fluids are mixed in the pore space (via Brie exponent). Inversion of rock frame properties from P-wave velocity with and without uncertainty is shown in Figure 1. 2D sections of the 3D model space constituted of dry bulk modulus $K_D$, dry shear modulus $G_D$ and porosity $\phi$ show the low misfit areas for each parameter (pink models). It is worth noting that the bulk and shear moduli show better fit than porosity. Comparing the cases without and with uncertainties on input velocity, the low misfit area is wider even if the convergence towards the true model is similar. That means that the average value for model parameters is similar but the associated standard deviation is larger when there is uncertainty on input. Inversion of $CO_2$ saturation and Brie exponent from P-wave velocity with and without uncertainty is shown in Figure 2. The well-known trade-off between saturation and Brie exponent is observed for both cases even if the the low misfit area is wider in case of uncertainty on input data.

A third sensitivity test is shown in Figure 3 where $CO_2$ saturation, Brie exponent and porosity from P-wave velocity and resistivity with and without uncertainty. Subagjo et al. (2018) present first tests of joint rock physics inversion at Sleipner combining FWI and CSEM inversion results. Adding resistivity input data helps to discriminate between fluid saturation and distribution but requires estimation of porosity in addition. Similarly to other sensitivity tests, using input data with uncertainty increases the standard deviation of each inverted parameters but the saturation and the porosity are less affected than the Brie exponent. Estimation of rock frame properties and of $CO_2$ saturation and Brie exponent for 1D profile are shown in Figure 4. These 1D log profiles are calculated from P-wave velocity with and without uncertainty. The mean values and the uncertainty ranges (+/- one standard deviation) of inverted parameters are plotted for both exact input data and velocity input $\pm 100\, m/s$. For both baseline (inversion of $K_D$, $G_D$ and $\phi$) and monitor (inversion of $S_{CO_2}$ and $e$) examples, it is important to note that the mean values are very close no matter if there is uncertainty on the input velocity or not. The uncertainty ranges slightly increase when the velocity uncertainty is included, more for shear modulus than porosity for baseline case. For the monitor case, this uncertainty range is larger at specific depths only for the case with uncertainty on input data. We notice also slight changes of the mean estimates at the same specific depths.

**Conclusions**

We derive an integrated formulation for propagation of uncertainty in the full imaging workflow used to quantify relevant $CO_2$ monitoring properties. In our two-step formulation, both inversion steps are formulated with Bayesian methods and the posterior uncertainty of the first step is used as prior data

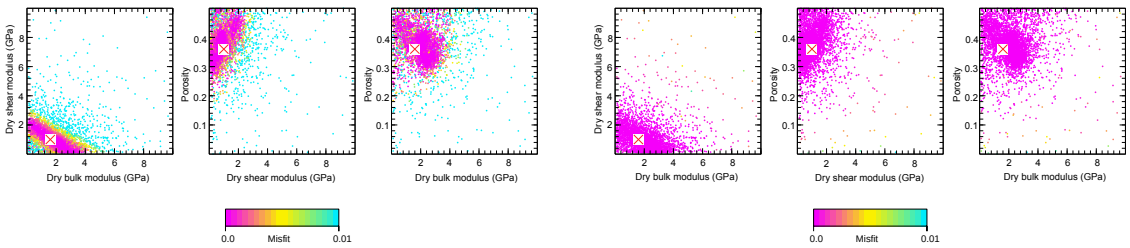


(a) No uncertainty on $V_P$ input (b) $\pm 100\ m/s$ uncertainty on $V_P$ input

***Figure 1*** *Inversion of dry bulk modulus $K_D$, dry shear modulus $G_D$ and porosity $\phi$ from P-wave velocity $V_P$ input with (a) no uncertainty and (b) $\pm 100\ m/s$ uncertainty. The figures give 2D sections of the 3D model space and each model is represented by a dot with a corresponding color giving the misfit value.*

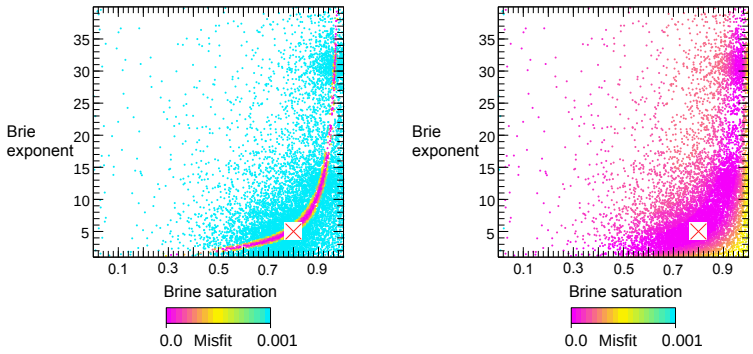


(a) No uncertainty on $V_P$ input (b) $\pm 100\ m/s$ uncertainty on $V_P$ input

***Figure 2*** *Inversion of $CO_2$ saturation $S_{CO_2}$ and Brie exponent e from P-wave velocity $V_P$ input with (a) no uncertainty and (b) $\pm 100\ m/s$ uncertainty. The figures give 2D sections of the 2D model space and each model is represented by a dot with a corresponding color giving the misfit value.*

uncertainty in the second step. The first sensitvity tests on seismic and CSEM data, both for baseline and monitor cases, show that the uncertainty range of inverted parameter increases when the input data is considered with uncertainty while the mean value stays similar. Globally, we can conclude that the rock physics inversion is quite stable with respect to uncertainty in input data. Other implementations to improve the integration of the two-steps workflow are going on.

## Acknowledgements

This work has been produced with support from the ACT Pre-ACT project (Project No. 271497) funded by RCN (Norway), Gassnova (Norway), BEIS (UK), RVO (Netherlands), and BMWi (Germany) and co-funded by the European Commission under the Horizon 2020 programme, ACT Grant Agreement No 691712. We also acknowledge the following industry partners for their contributions: Total, Statoil, Shell, TAQA. Malcolm Sambridge is acknowledge for providing the NA tools.

## References

Biot, M. [1956] Theory of propagation of elastic waves in a fluid-saturated porous solid - I. Low-frequency range, II. Higher frequency range. *Journal of Acoustical Society of America*, **28**, 168–178.

Brie, A., Pampuri, F., Marsala, A. and Meazza, O. [1995] Shear sonic interpretation in gas-bearing sands. *SPE Annual Technical Conf. 30595*, 701–710.

Dupuy, B., Garambois, S. and Virieux, J. [2016] Estimation of rock physics properties from seismic attributes - Part I: Strategy and sensitivity analysis. *Geophysics*, **81**(3), 35–53.

Dupuy, B., Romdhane, A., Eliasson, P., Querendez, E., Yan, H., Torres, V. and Ghaderi, A. [2017]

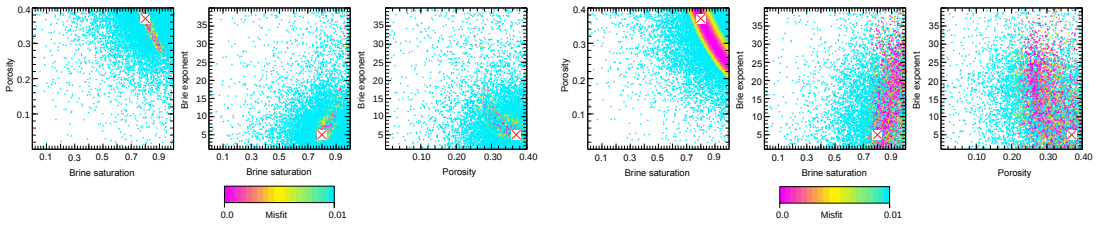


(a) No uncertainty on $V_P$ and $R_t$ inputs

(b) $\pm 100\ m/s$ and $\pm 5\ \Omega.m$ uncertainties on $V_P$ and $R_t$ inputs

***Figure 3*** *Inversion of $CO_2$ saturation $S_{CO_2}$, Brie exponent $e$ and porosity $\phi$ from P-wave velocity $V_P$ and resistivity $R_t$ inputs with (a) no uncertainty and (b) $\pm 100\ m/s$ uncertainty on $V_P$ and $\pm 5\ \Omega.m$ uncertainty on $R_t$. The figures give 2D sections of the 3D model space and each model is represented by a dot with a corresponding color giving the misfit value.*

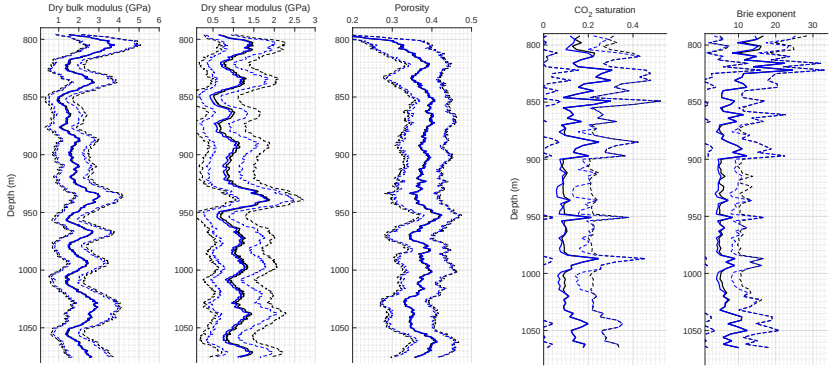


(a) Baseline results

(b) Monitor results

***Figure 4*** *(a) Inversion of dry bulk modulus $K_D$, dry shear modulus $G_D$ and porosity $\phi$ and (b) inversion of $CO_2$ saturation $S_{CO_2}$ and Brie exponent $e$. Continuous blue lines stand for results with no uncertainty on $V_P$ input while continuous black lines stand for results with $\pm 100\ m/s$ uncertainty on $V_P$ input. The dashed lines gives the ranges of uncertainty for each inverted parameters i.e. $\pm$ one standard deviation.*

Quantitative seismic characterization of $CO_2$ at the Sleipner storage site, North Sea. *Interpretation*, **5**(4), SS23–SS42.

Eliasson, P. and Romdhane, A. [2017] Uncertainty evaluation in waveform-based imaging methods - A case study at Sleipner. In: *79th EAGE Conference and Exhibition 2017*.

Gassmann, F. [1951] Über die elastizität poröser medien. *Vierteljahrsschrift der Naturforschenden Gesellschaft in Zurich*, **96**, 1–23.

Ghosh, R., Sen, M.K. and Vedanti, N. [2015] Quantitative interpretation of $CO_2$ plume from Sleipner (North Sea),using post-stack inversion and rock physics modeling. *International Journal of Greenhouse Gas Control*, **32**, 147–158.

Romdhane, A. and Querendez, E. [2014] $CO_2$ characterization at the Sleipner field with full waveform inversion: application to synthetic and real data. *Energy Procedia*, **63**, 4358–4365.

Sambridge, M.S. [1999a] Geophysical inversion with a neighbourhood algorithm - I. Searching a parameter space. *Geophysical Journal International*, **138**, 479–494.

Sambridge, M.S. [1999b] Geophysical inversion with a neighbourhood algorithm - II. Appraising the ensemble. *Geophysical Journal International*, **138**, 727–746.

Subagjo, I., Dupuy, B., Park, J., Romdhane, A. and Stovas, A. [2018] Joint rock physics inversion of seismic and EM data for CO2 monitoring at Sleipner. In: *EAGE Near surface Geoscience*.

Tarantola, A. [2005] *Inverse Problem theory and methods for model parameter estimation*. Society for Industrial and Applied Mathematics, Philadelphia.